AIP Journal of Applied Physics

Conversion mechanism of conductivity of phosphorus-doped ZnO films induced by post-annealing

Jichao Li, Bin Yao, Yongfeng Li, Zhanhui Ding, Ying Xu, Ligong Zhang, Haifeng Zhao, and Dezhen Shen

Citation: Journal of Applied Physics **113**, 193105 (2013); doi: 10.1063/1.4805778
View online: http://dx.doi.org/10.1063/1.4805778
View Table of Contents: http://scitation.aip.org/content/aip/journal/jap/113/19?ver=pdfcov
Published by the AIP Publishing

Conversion mechanism of conductivity of phosphorus-doped ZnO films induced by post-annealing

Jichao Li,[1,2] Bin Yao,[1,2,a)] Yongfeng Li,[1] Zhanhui Ding,[2] Ying Xu,[2] Ligong Zhang,[3] Haifeng Zhao,[3] and Dezhen Shen[3]
[1]*Key Laboratory of Physics and Technology for Advanced Batteries, Ministry of Education and Department of Physics, Jilin University, Changchun 130023, People's Republic of China*
[2]*State Key Laboratory of Superhard Materials and College of Physics, Jilin University, Changchun 130023, People's Republic of China*
[3]*State Key Laboratory of Luminescence and Applications, Changchun Institute of Optics, Fine Mechanics and Physics, Chinese Academy of Sciences, No. 3888 Dongnanhu Road, Changchun 130033, People's Republic of China*

(Received 19 December 2012; accepted 1 May 2013; published online 20 May 2013)

The effects of post-annealing on conductivity of phosphorus-doped ZnO (PZO) films grown at 500 °C by radio frequency magnetron sputtering are investigated in a temperature ranging from 600 °C to 900 °C. The as-grown PZO exhibits *n*-type conductivity with an electron concentration of $1.19 \times 10^{20}\,cm^{-3}$, and keeps *n*-type conductivity as annealed at 600 °C-700 °C but electron concentration decreases with increasing temperature. However, it converts to *p*-type conductivity as annealed at 800 °C. Further increasing temperature, it still shows *p*-type conductivity but the hole concentration decreases. It is found that the P occupies mainly Zn site (P_{Zn}) in the as-grown PZO, which accounts for good *n*-type conductivity of the as-grown PZO. The amount of the P_{Zn} decreases with increasing temperature, while the amount of Zn vacancy (V_{Zn}) increases from 600 °C to 800 °C but decreases greatly at 900 °C, resulting in that the amount of P_{Zn}-$2V_{Zn}$ complex increases with increasing temperature up to 800 °C but decreases above 800 °C. It is suggested that the P_{Zn}-$2V_{Zn}$ complex acceptor is responsible for *p*-type conductivity, and that the conversion of conductivity is due to the change of the amount of the P_{Zn} and P_{Zn}-$2V_{Zn}$ with annealing temperature. © *2013 AIP Publishing LLC*. [http://dx.doi.org/10.1063/1.4805778]

I. INTRODUCTION

ZnO is considered as a promising material for next-generation ultraviolet (UV) light emitting diodes (LEDs) and lasing diodes (LD) because of its wide band gap of 3.37 eV and large exciton binding energy of 60 meV at room temperature.[1,2] However, lack of stable and reproducible *p*-type ZnO has been an obstacle for application of ZnO in optoelectronic devices. Based on simple valence electron arguments, a natural doping approach for *p*-type ZnO is to use group-V elements such as P. In recent years, many approaches and techniques have been used to fabricate *p*-type phosphorus-doped ZnO (PZO) films.[3–8] More encouragingly, LEDs based on *p*-type PZO also are reported.[9,10] However, similar to other dopants, the *p*-type PZO also suffers the instability problem, that is, it can convert to *n*-type after kept in air for some period of time, which has been key scientific problem of optoelectronic application of ZnO. In order to resolve this problem, it is necessary to understand well the formation mechanism of *p*-type PZO. However, it has been argued up to now which defect or defect complex should be responsible for the *p*-type conductivity observed in the PZO. Some researchers ascribe *p*-type conductivity to P_O acceptor,[11,12] while others attribute it to P_{Zn}-$2V_{Zn}$ acceptor complex.[13–15] Obviously, characterization of chemical states of P in ZnO as well as of intrinsic defects of ZnO is important for us to understand mechanism of *p*-type conductivity in the PZO and find effective approaches to promote stability of *p*-type PZO.

In the present work, we prepared PZO films by radio frequency (RF) magnetron sputtering and post-annealing technique and investigated the change of conductivity of the PZO with annealing temperature, and discussed the change mechanism by characterization of chemical states of P and of the intrinsic defects of ZnO at various annealing temperatures.

II. EXPERIMENTAL

Undoped ZnO and PZO films were deposited on quartz substrates by RF magnetron sputtering of ZnO and PZO ceramic targets, respectively. The ZnO and PZO targets were fabricated by sintering high purity ZnO (99.99%) and the mixture of the ZnO and P_2O_5 (99.998%) powder, respectively. The nominal concentration of phosphorus in PZO target was 2 at. %. To eliminate influence of oxygen, the vacuum chamber was evacuated to a base pressure of 5×10^{-4} pa prior to deposition, and then filled with high pure Ar (99.999%) to 1.0 Pa, which is kept during depositing process. All films were sputtered for 2 h at substrate temperature of 500 °C. The as-grown films with 1 cm × 1 cm size were cut into four square pieces and then rapidly annealed at different temperatures in the range of 600–900 °C in steps of 100 °C under 10^{-4} Pa in a tube furnace.

The crystal structures of samples were characterized by x-ray diffraction (XRD) with $Cu_{K\alpha 1}$ radiation ($\lambda = 0.15406$ nm), the scan step used is 0.02°, and error is within ±0.0003 nm for lattice constant measurement. The electrical properties were measured in the van der Pauw configuration by a Hall measurement system at room temperature. The temperature-dependent

a)E-mail: binyao@jlu.edu.cn

photoluminescence (PL) was performed using the UV Labran Infinity Spectrophotometer with He–Cd laser line of 325 nm as an excitation source. The chemical states of elements were analyzed by x-ray photoelectron spectroscopy (XPS).

III. RESULTS AND DISCUSSION

Fig. 1(a) shows the XRD patterns collected from the PZO films annealed at different temperatures. Only strong (002) and weak (004) diffraction peaks are observed, and no diffraction peak of other phases, such as Zn_3P_2 or P_2O_5, is detected, implying that P atoms incorporate into the lattice of ZnO to form PZO films with hexagonal structure and (002) preferential orientation. Lattice constant in *c* axis of the PZO is calculated using the XRD data and plotted as a function of annealing temperature, as shown in Fig. 1(b). One can see that the lattice constant *c* monotonically increases as annealing temperature increases from 600 °C to 900 °C. In order to eliminate impact of the strain induced by thermal mismatch and lattice mismatch, the undoped ZnO film is annealed at 600 °C and 800 °C, and their lattice constant *c* is calculated to be 0.5212 and 0.5210 nm shown in Fig. 1(b), respectively, which is very close to 0.5209 nm of bulk ZnO,[16] implying that the strain is almost relaxed in the annealing temperature range. Therefore, the increase of lattice constant *c* of the PZO not arises from the strain but the P doping. It is noted that the lattice constant *c* of the PZO is smaller than that of bulk ZnO at the annealing temperature below 850 °C but larger than that of bulk ZnO at the annealing temperature above 850 °C. It is known that the ionic radii of P^{5+} (0.031–0.034 nm) and P^{3+} (0.044–0.058 nm) are smaller than that of Zn^{2+} (0.074 nm), while the ionic radius of P^{3-} (0.18–0.212 nm) is larger than that of O^{2-} (0.138–0.14 nm). So, the substitution of P for Zn (P_{Zn}) can lead to decrease of the lattice constant *c*, while substitution of P for O (P_O) can result in increase of the lattice constant *c*. Based on the XRD results and discussions mentioned above, it is deduced that most of P atoms should occupy Zn sites when the PZO is annealed at the temperatures below 850 °C but O sites when the PZO is annealed at temperatures above 850 °C. Therefore, the *c*-axis lattice expansion is due to the gradual decrease of the amount of P_{Zn} with increasing annealing temperature. The origin of decrease of P_{Zn} is not clear yet, we speculate that it may be related to the conversion of P doping configurations from P_{Zn} to P_O.[17]

Table I displays the electrical properties of the undoped ZnO and PZO films. The as-grown undoped ZnO exhibits *n*-type conductivity with an electron concentration of $6.23 \times 10^{16}\,cm^{-3}$, which is a common feature for an undoped ZnO due to the existence of native donor defects such as interstitial zinc (Zn_I) and oxygen vacancies (V_O). However, the conductivity measured for the 600 °C-annealed undoped ZnO is ambiguous, suggesting that native acceptors such as V_{Zn} have been considerably formed and compete with the native donors. As annealing temperature increases from 700 °C to 900 °C, the undoped ZnO films return to *n*-type conductivity due to that native donors, such as V_O, dominate again, and the electron concentration monotonically increases from 5.37×10^{17} to $1.69 \times 10^{18}\,cm^{-3}$. However, for the as-grown PZO, it exhibits good *n*-type conductivity with an electron concentration up to $1.19 \times 10^{20}\,cm^{-3}$, much higher than that of the as-grown undoped ZnO. It is well known that P has amphoteric nature of substitution for Zn or O when it is doped in ZnO and behaves as acceptor when it substitutes for O site (P_O) but triple donor when it replaces Zn site (P_{Zn}).[8] Obviously, so high electron concentration in as-grown PZO compared to as-grown undoped ZnO indicates that most of P atoms occupy Zn sites in the as-grown PZO film, in agreement with the result of XRD.[18] As annealed in the temperature range from 600 °C to 700 °C, the PZO film still shows *n*-type conduction, but the electron concentration monotonically

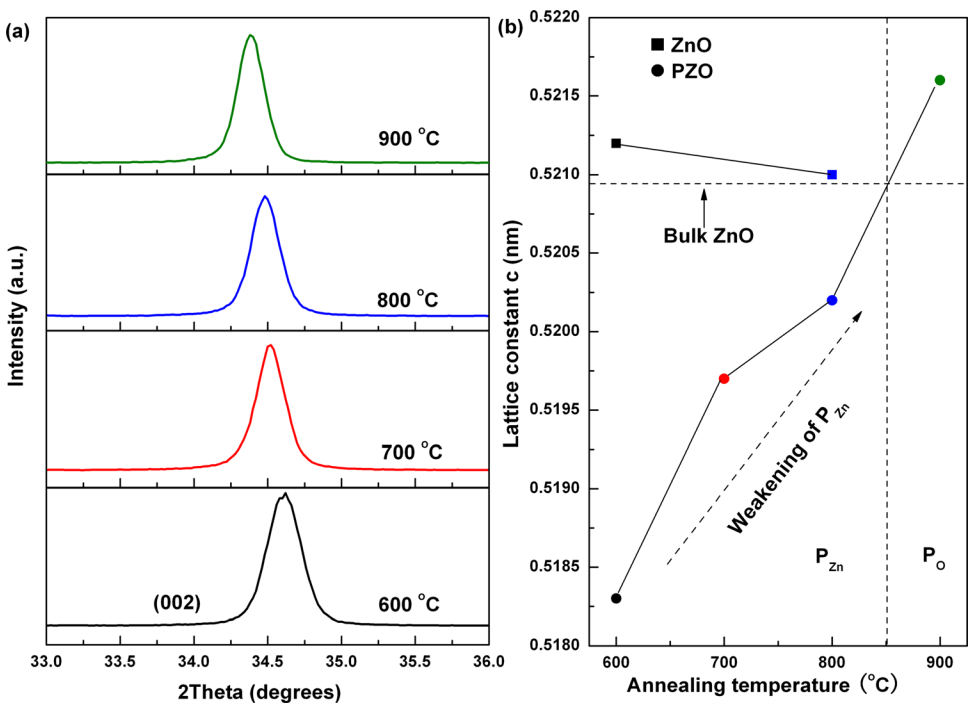

FIG. 1. (a) Typical XRD spectrum of PZO films annealed at different temperatures. (b) Lattice constant *c* of PZO films as a function of annealing temperature.

TABLE I. Electrical properties of undoped ZnO and PZO films measured by van der Pauw method at room temperature.

Sample	Annealing temp. (°C)	Resistivity (Ω cm)	Mobility ($cm^2\ V^{-1}\ s^{-1}$)	Carrier density (cm^{-3})	Type
ZnO	as-grown	97.9	1.03	6.23×10^{16}	n
ZnO	600	63.5	…	…	p/n
ZnO	700	13.8	1.45	5.37×10^{17}	n
ZnO	800	3.37	2.96	6.40×10^{17}	n
ZnO	900	1.15	3.28	1.69×10^{18}	n
PZO	as-grown	5.95×10^{-2}	0.88	1.19×10^{20}	n
PZO	600	0.57	0.78	1.40×10^{19}	n
PZO	700	8.04	1.5	5.29×10^{17}	n
PZO	800	64.2	2.82	3.81×10^{16}	p
PZO	900	1.59×10^{3}	4.82	1.16×10^{13}	p

decreases from 1.19×10^{20} to $5.29 \times 10^{17}\,cm^{-3}$, which is different from annealing-temperature dependent electron concentration of the undoped ZnO. It is evident that the decrease of the electron concentration should be related to the decrease of the amount of P_{Zn} donors based on the XRD results. Interestingly, the conversion of conductivity from *n*- to *p*-type happens as the PZO is annealed at temperatures of 800 and 900 °C, and corresponding hole concentration is $3.81 \times 10^{16}\,cm^{-3}$ and $1.16 \times 10^{13}\,cm^{-3}$, respectively. From the Hall measurement, it can be seen that 800 °C annealing favors to obtain *p*-type PZO with good electrical properties.

To understand the conversion mechanism, low-temperature PL measurement is performed for the undoped ZnO and PZO films. Fig. 2 shows the 83 K PL spectra of the undoped ZnO films annealed at different temperatures. The prominent emission peak centered at 3.363 eV can be assigned to the donor-bound exciton radiative recombination (D^0X) and the 3.379 eV peak is usually associated with free exciton (FX).[19–21] The appearance of FX, in general, is the indication of good crystalline of the films.[20] The emission peak at 3.313 eV has been ascribed to the transition of conduction band electron to acceptor located in basal plane stacking faults in some literatures published previously.[22,23]

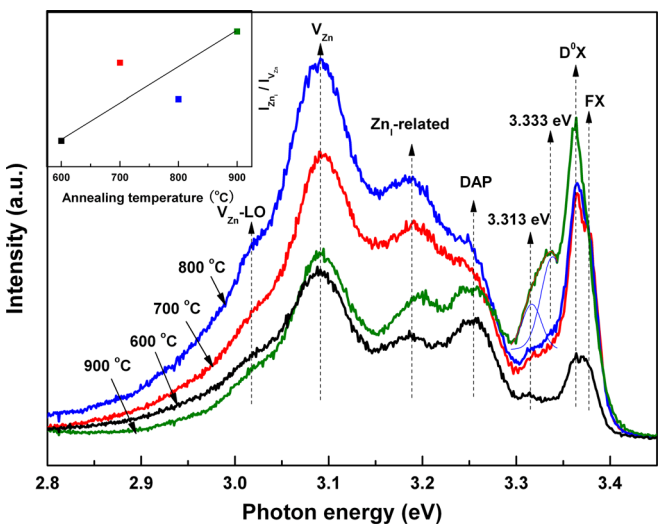

FIG. 2. 83 K PL spectra of undoped ZnO films annealed at different temperatures. The inset shows the intensity ratio of Zn_I-related to V_{Zn} peaks as a function of annealing temperatures.

The 3.188 eV peak is similar to the peak observed previously by Sann *et al.*[24] in ZnO powders annealed in ammonia atmosphere (3.193 eV), and is attributed to the transition associated with interstitial Zn based on electron paramagnetic resonance measurements. The most prominent emission peak at 3.090 eV is usually considered as the transition of electron from conduction-band to V_{Zn} ((e, V_{Zn})).[25–29] Appearance of so strong peak indicates that considerable V_{Zn} exists in the annealed undoped ZnO. The peak at 3.017 eV is ascribed to longitudinal optical (LO) phonon replica of (e, V_{Zn}) due to that the energy difference between the two peak is close to the LO phonon energy of 72 meV. Other interesting emission peak at 3.252 eV is due to the recombination of donor-acceptor pair (DAP). One can see that the intensity of the 3.313 eV emission peak dramatically increases and an additional emission peak at 3.333 eV emerges in the spectrum of 900 °C-annealed ZnO. There are many kinds of explanation about the origin of the 3.333 eV peak up to now, two of which are accepted widely. One ascribes the peak to the two electron satellite (TES) of D^0X,[30] and another assigns the peak to the recombination of exciton bound to V_{Zn} located in grain boundaries.[31] It should be noted that the appearance of the 3.333 eV peak is accompanied with the dramatical increase of the intensity of the 3.313 eV peak. In general, these stacking faults can promote the formation of grain boundaries. Therefore, the positive correlation between the 3.333 eV and 3.313 eV emission peaks suggests that the 3.333 eV peak likely arises from the transition of excitons bound to V_{Zn} located in grain boundaries. Moreover, the 3.333 eV emission peak is also observed in the spectrum of 900 °C-annealed PZO, where no D^0X reveals (as shown in Fig. 3), confirming that the 3.333 eV emission should not originate from TES of D^0X but the recombination of excitons bound to V_{Zn} in the present case.

It should be noticed that the intensity of the V_{Zn} peak increases steeply as annealing temperature increases up to 800 °C but decreases drastically at 900 °C, as shown in Fig. 2. This indicates that the amount of V_{Zn} acceptor increases with increasing annealing temperature from 600 °C to 800 °C and then decrease at 900 °C. If the amount of donors in the films does not change with annealing temperature, the increase of the amount of the V_{Zn} should lead to that electron concentration decreases with increasing annealing temperature from 600 to 800 °C and then increases at 900 °C, which is

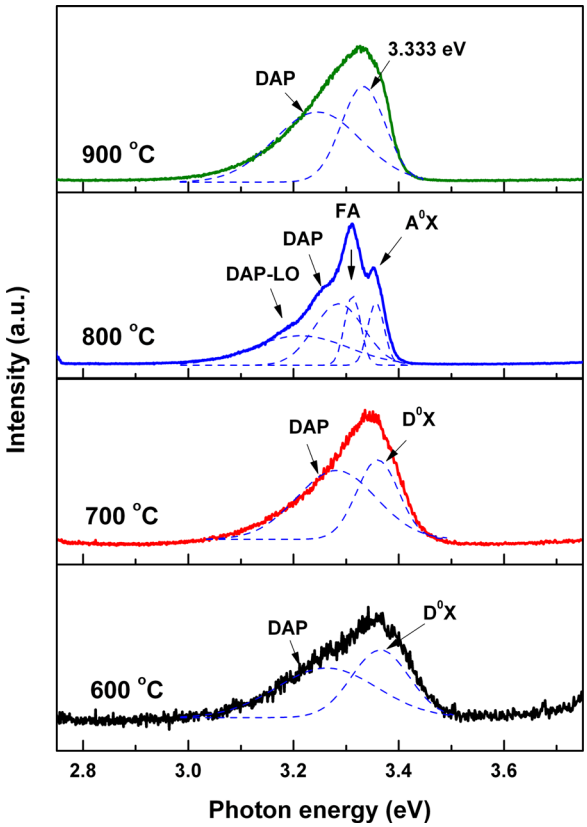

FIG. 3. 83 K PL spectra of PZO films annealed at different temperatures.

inconsistent with the variation of electron concentration shown in Table I. This implies that some donor is generated and the amount of the donor increases with annealing temperature. In fact, one can see from Fig. 2 that the 3.188 eV emission peak, which is considered to be related to Zn_I-related donors, becomes stronger and stronger with increasing annealing temperature, implying that the amount of Zn_I-related donors increases with increasing annealing temperature. In our previous work,[32] it was found that Zn atoms started to escape from ZnO and generate V_{Zn} at annealing temperature of 600 °C. Some of the escaped Zn atoms leave the ZnO film, and others inevitably remain in the ZnO films to form Zn_I-related donors. It has been suggested that the 3.090 eV emission peak arises from the transition of electron from conduction band to V_{Zn} while the 3.188 eV emission peak is owing to the transition of electron from Zn_I-related donor to valence band. Therefore, it is not difficult to conclude that the ionization energy of the V_{Zn} is 98 meV higher than that of the Zn_I-related donor. So, the electric properties of the undoped ZnO are dominated by Zn_I-related donors in the annealing temperature range, though the amount of both V_{Zn} and Zn_I increases with increasing annealing temperature. The intensity ratio of Zn_I-related to V_{Zn} peaks as a function of annealing temperature is more explicitly shown in the inset of Fig. 2, indicating that the ratio almost linearly increases with increasing annealing temperature. Consequently, the electron concentration gradually increases with increasing annealing temperature.

Fig. 3 shows the 83 K PL spectra of the PZO films annealed at various temperatures. For the 600 °C-annealed PZO, the spectrum can be fitted well with two emission peaks located at 3.365 eV and 3.263 eV using Gaussian fitting method. The dominant emission peak at 3.365 eV can be assigned to D^0X,[33] and the broad emission peak at 3.263 eV to the recombination of DAP.[33] For 700 °C-annealed PZO, the spectrum is also dominated by the D^0X and the DAP transition. This implies that donor is dominant in the PZO annealed at 600 °C and 700 °C, in agreement with *n*-type conductivity of the two samples shown in Table I. However, for the 800 °C-annealed PZO, the spectrum composes of four emission bands, located at 3.356, 3.310, 3.286, and 3.213 eV, respectively. The emission peak at 3.356 eV is attributed to the acceptor-bound exciton radiative recombination (A^0X),[6,34] which is different from D^0X observed in the *n*-type PZO prepared by annealing at 600 °C and 700 °C, implying that acceptor is dominant in the 800 °C-annealed PZO. In addition, two additional strong emission peaks located at 3.310 and 3.213 eV, respectively, are observed in the 800 °C-annealed PZO compared to 600 °C and 700 °C-annealed PZO. The 3.310 eV peak is usually assigned to the transition of free electron from conduction band to acceptor level (FA) related to phosphorus acceptor.[6,34] The emission peak located at 3.286 eV in the 800 °C-annealed PZO is ascribed to the DAP transition, while the 3.213 eV peak can be assigned to DAP-LO due to that the energy difference between the two peaks is close to the LO phonon energy of 72 meV.

To confirm the assignment of the 3.310 eV peak, temperature-dependent PL is performed for the 800 °C-annealed PZO, as shown in Fig. 4. One can see that the 3.310 eV emission peak shows a continuous red-shift with increasing measurement temperatures, and overlaps with FX to form a broad emission band at room temperature, which is a typical characteristic of FA transition. As shown in the inset of Fig. 4, the temperature-dependent photon energy of the FA transition is fitted well by following equation:

$$E_{FA}(T) = E_g(T) - E_A + k_B T/2, \quad (1)$$

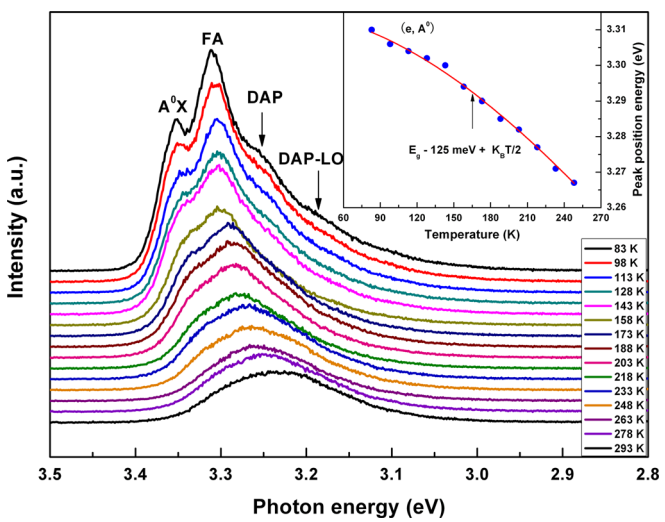

FIG. 4. Temperature-dependent PL spectra of 800 °C-annealed PZO film. The inset shows the temperature-dependent peak energy of FA and the fitting curve using Eq. (1) for 800 °C-annealed PZO film.

where E_{FA} (T) is the temperature-dependent the FA transition energy, E_g (T) is the band gap energy, E_A is the acceptor energy level, and k_B is the Boltzmann constant. The acceptor energy level is estimated to be 125 meV, well consistent with the previous report.[15] For the 900 °C-annealed PZO, there are two emission peaks centered at 3.333 eV and 3.246 eV in the PL spectrum and no A^0X and FA are observed, as shown in Fig. 3. Similar to the 900 °C-annealed undoped ZnO, the 3.330 eV emission peak is related to V_{Zn} located in grain boundaries and the emission peak at 3.246 eV is likely related to the DAP transition.[33]

To further identify the acceptor involved in the FA, XPS measurement is performed for the 800 °C-annealed PZO, as shown in Fig. 5. The XPS spectrum exhibits clearly two peaks located at 139.28 and 133.25 eV. The peak with binding energy of 139.28 eV originates from the Zn_{3s} signal from Zn-O bond in ZnO.[35] The P_{2p} at a binding energy of 133.5–133.7 eV has been suggested to come from PO_4 ion in the film.[36] Therefore, the 133.25 eV peak is assigned to the P_{2p} from PO_4 ion. This indicates that the P occupies mainly Zn sites and forms tetrahedral bonds with O in the PZO, consistent with the XRD results, implying that the phosphorus-related acceptor involved in the FA is not P_O but P_{Zn}-$2V_{Zn}$ complex acceptor,[13–15] which is responsible for *p*-type conductivity of the PZO.

Based on the XRD and PL results mentioned above, the Hall measurement results of the PZO can be explained well as following: for the as-grown PZO, P occupies mainly Zn site to form triple donors, leading to its *n*-type conductivity with high electron concentration. Since the amount of the P_{Zn} decreases with increasing annealing temperature while the amount of V_{Zn} increases first up to 800 °C and then decreases, the amount of the P_{Zn}-$2V_{Zn}$ complex acceptor may increase first with increasing temperature up to 800 °C and then decrease after 800 °C. When the PZO is annealed at 600 and 700 °C, the P_{Zn} is dominant due to that only a small amount of P_{Zn}-$2V_{Zn}$ form, so the conductivity is still *n*-type, but the electron concentration decreases with increasing temperature due to decrease in the amount of the P_{Zn} and increase in the amount of the P_{Zn}-$2V_{Zn}$ complex acceptor. When the PZO annealed at 800 °C, the amount of the P_{Zn}-$2V_{Zn}$ reaches maximum and much larger than that of the P_{Zn}, resulting in that the conductivity of the PZO converts from *n*-type to *p*-type. Further increasing annealing temperature to 900 °C, the amount of the P_{Zn}-$2V_{Zn}$ decreases, leading to decrease in the hole concentration of the *p*-type PZO.

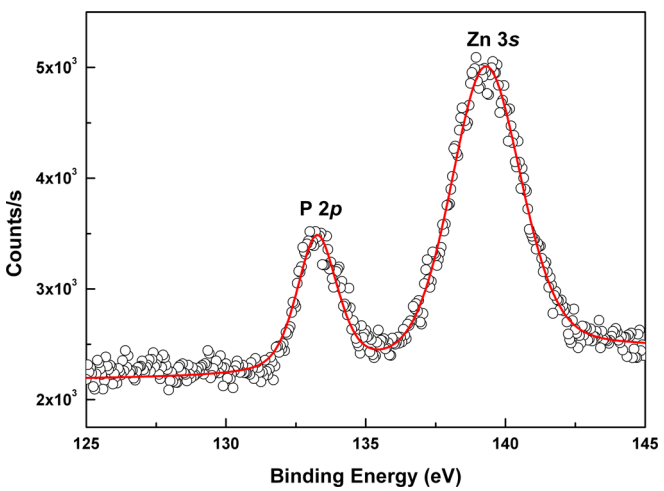

FIG. 5. XPS spectra and fitting curve of 800 °C-annealed PZO film.

IV. CONCLUSIONS

By using RF magnetron sputtering, phosphorus-doped ZnO films are grown on quartz at a substrate temperature of 500 °C and then annealed in the temperature range from 600 °C to 900 °C. The as-grown PZO film is *n*-type and keeps *n*-type at the annealing temperatures of 600–700 °C, but converts to *p*-type after 800 °C annealing. Further increasing annealing temperature, it still shows *p*-type conductivity but the hole concentration decreases. The P occupies mainly Zn site (P_{Zn}) in the as-grown PZO, which accounts for good *n*-type conductivity of the as-grown PZO. The amount of the P_{Zn} decreases with increasing temperature, while the amount of V_{Zn} increases from 600 °C to 800 °C but decreases greatly at 900 °C, resulting in that the amount of P_{Zn}-$2V_{Zn}$ complex increases with increasing temperature up to 800 °C but decreases above 800 °C. The *p*-type conductivity of the PZO is due to the P_{Zn}-$2V_{Zn}$ complex acceptor, and ionization energy of which is estimated to be 125 meV. The conversion of the conductivity is attributed to the change of the amount of the P_{Zn} and P_{Zn}-$2V_{Zn}$ complex with annealing temperature.

ACKNOWLEDGMENTS

This work was supported by the National Natural Science Foundation of China under Grant Nos. 10874178, 11074093, 61205038, and 11274135, Natural Science Foundation of Jilin province under Grant No. 201115013, and National Found for Fostering Talents of Basic Science under Grant No. J1103202.

[1]D. C. Look, D. C. Reynolds, J. W. Hemsky, R. L. Jones, and J. R. Sizelove, Appl. Phys. Lett. **75**, 811 (1999).
[2]Z. K. Tang, G. K. L. Wong, P. Yu, M. Kawasaki, A. Ohtomo, H. Koinuma, and Y. Segawa, Appl. Phys. Lett. **72**, 3270 (1998).
[3]K. K. Kim, H. S. Kim, D. K. Hwang, J. H. Lim, and S. J. Park, Appl. Phys. Lett. **83**, 63 (2003).
[4]V. Vaithianathan, B. T. Lee, and S. S. Kim, J. Appl. Phys. **98**, 043519 (2005).
[5]F. X. Xiu, Z. Yang, L. J. Mandalapu, and J. L. Liu, Mater. Res. Soc. Symp. Proc. **892**, 0892-FF18-09-EE09-09 (2005).
[6]D. K. Hwang, H. S. Kim, J. H. Lim, J. Y. Oh, J. H. Yang, S. J. Park, K. K. Kim, D. C. Look, and Y. S. Park, Appl. Phys. Lett. **86**, 151917 (2005).
[7]F. X. Xiu, Z. Yang, L. J. Mandalapu, and J. L. Liu, Appl. Phys. Lett. **88**, 152116 (2006).
[8]A. Allenic, W. Guo, Y. B. Chen, M. B. Katz, G. Y. Zhao, Y. Che, Z. D. Hu, B. Liu, S. B. Zhang, and X. Q. Pan, Adv. Mater. **19**, 3333 (2007).
[9]J. H. Lim, C. K. Kang, K. K. Kim, I. K. Park, D. K. Hwang, and S. J. Park, Adv. Mater. **18**, 2720 (2006).
[10]H. S. Kim, F. Lugo, S. J. Pearton, D. P. Norton, Y. L. Wang, and F. Ren, Appl. Phys. Lett. **92**, 112108 (2008).
[11]M. S. Oh, D. K. Hwang, Y. S. Choi, J. W. Kang, S. J. Park, C. S. Hwang, and K. I. Cho, Appl. Phys. Lett. **93**, 111905 (2008).
[12]D. K. Hwang, M. S. Oh, J. H. Lim, C. G. Kang, and S. J. Park, Appl. Phys. Lett. **90**, 021106 (2007).

[13]W. J. Lee, J. Kang, and K. J. Chang, Phys. Rev. B **73**, 024117 (2006).
[14]H. S. Kim, S. J. Pearton, D. P. Norton, and F. Ren, J. Appl. Phys. **102**, 104904 (2007).
[15]A. Allenic, W. Guo, Y. B. Chen, Y. Che, Z. D. Hu, B. Liu, and X. Q. Pan, J. Phys. D: Appl. Phys. **41**, 025103 (2008).
[16]PDF card No. 80-0075.
[17]H. F. Liu and S. J. Chua, Appl. Phys. Lett. **96**, 091902 (2010).
[18]Y. W. Heo, S. J. Park, K. Lp, S. J. Pearton, and D. P. Norton, Appl. Phys. Lett. **83**, 1128 (2003).
[19]L. J. Wang and N. C. Giles, J. Appl. Phys. **94**, 973 (2003).
[20]P. Misra, T. K. Sharma, and L. M. Kukreja, Curr. Appl. Phys. **9**(1), 179 (2009).
[21]M. Ding, D. X. Zhao, B. Yao, B. H. Li, Z. Z. Zhang, and S. D. Zhen, Appl. Phys. Lett. **98**, 062102 (2011).
[22]M. Schirra, R. Schneider, A. Reiser, G. M. Prinz, M. Feneberg, J. Biskupek, U. Kaiser, C. E. Krill, R. Sauer, and K. Thonke, Physica B **401–402**, 362–365 (2007).
[23]M. Schirra, R. Schneider, A. Reiser, G. M. Prinz, M. Feneberg, J. Biskupek, U. Kaiser, C. E. Krill, K. Thonke, and R. Sauer, Phys. Rev. B **77**, 125215 (2008).
[24]J. Sann, J. Stehr, A. Hofstaetter, D. M. Hofmann, A. Neumann, M. Lerch, U. Haboeck, A. Hoffmann, and C. Thomsen, Phys. Rev. B **76**, 195203 (2007).
[25]T. V. Butkhuzi, A. V. Bureyev, A. N. Georgobiani, N. P. Kekelidze, and T. G. Khulordava, J. Cryst. Growth **117**, 366 (1992).
[26]A. N. Georgobiani, M. B. Kotlyarevskii, V. V. Kidalov, L. S. Lepnev, and I. V. Rogozin, Inorg. Mater. **37**, 1095–1098 (2001).
[27]X. L. Wu, G. G. Siu, C. L. Fu, and H. C. Ong, Appl. Phys. Lett. **78**, 2285 (2001).
[28]S. H. Jeong, B. S. Kim, and B. T. Lee, Appl. Phys. Lett. **82**, 2625 (2003).
[29]Y. R. Sui, B. Yao, Z. Hua, G. Z. Xing, X. M. Huang, T. Yang, L. L. Gao, T. T. Zhao, H. L. Pan, H. Zhu, and T. Wu, J. Phys. D: Appl. Phys. **42**, 065101 (2009).
[30]A. Teke, U. Ozgur, S. Dogan, X. Gu, H. Morkoç, B. Nemeth, J. Nause, and H. O. Everitt, Phys. Rev. B **70**, 195207 (2004).
[31]V. S. Yalishev, Y. S. Kim, X. L. Deng, B. H. Park, and S. U. Yuldashev, J. Appl. Phys. **112**, 013528 (2012).
[32]G. Z. Xing, B. Yao, C. X. Cong, T. Yang, Y. P. Xie, B. H. Li, and D. Z. Shen, J. Alloys Compd. **457**, 36–41 (2008).
[33]A. Allenic, X. Q. Pan, Y. Che, Z. D. Hu, and B. Liu, Appl. Phys. Lett. **92**, 022107 (2008).
[34]D. K. Hwang, M. S. Oh, Y. S. Choi, and S. J. Park, Appl. Phys. Lett. **92**, 161109 (2008).
[35]C. D. Wagner, W. M. Riggs, L. E. Davis, J. F. Moulder, and G. E. Muilenberg, *Handbook of X-ray Photoelectron Spectroscopy* (Perkin-Elmer, Eden Prairie, MN, 1979), p. 54.
[36]J. F. Moulder, W. F. Stickle, P. E. Sobol, and K. D. Bomben, *Handbook of X-Ray Photoelectron Spectroscopy* (Perkin-Elmer, Minnesota, 1992).